Identification of optimal parameter combinations for the emergence of bistability

Physical Biology

PAPER

Identification of optimal parameter combinations for the emergence of bistability

Imre Májer, Amirhossein Hajihosseini and Attila Becskei[1]

Computational and Systems Biology, Biozentrum, University of Basel, Klingelbergstr. 50/70, Basel, Switzerland

[1] Author to whom any correspondence should be addressed.

E-mail: attila.becskei@unibas.ch

Keywords: ultrasensitivity, feedback, gene regulatory network

OPEN ACCESS

RECEIVED
19 May 2015

REVISED
22 October 2015

ACCEPTED FOR PUBLICATION
23 October 2015

PUBLISHED
23 November 2015

Abstract

Bistability underlies cellular memory and maintains alternative differentiation states. Bistability can emerge only if its parameter range is either physically realizable or can be enlarged to become realizable. We derived a general rule and showed that the bistable range of a reaction parameter is maximized by a pair of other parameters in any gene regulatory network provided they satisfy a general condition. The resulting analytical expressions revealed whether or not such reaction pairs are present in prototypical positive feedback loops. They are absent from the feedback loop enclosed by protein dimers but present in both the toggle-switch and the feedback circuit inhibited by sequestration. Sequestration can generate bistability even at narrow feedback expression range at which cooperative binding fails to do so, provided inhibition is set to an optimal value. These results help to design bistable circuits and cellular reprogramming and reveal whether bistability is possible in gene networks in the range of realistic parameter values.

1. Introduction

Bistability is the co-existence of two stable equilibria. It is a hallmark of self-organization in dynamical systems, and has a wide range of occurrence and applications [1–3].

Bistability creates two distinct cell states or phenotypes in genetically identical cells. It can also store memory of past stimuli by hysteresis and promote cell-cycle oscillations [4, 5]. These effects underlie cellular differentiation, adaptation to varying environments by bet hedging, and may have practical implications for cellular reprogramming and antibiotic resistance [6–10].

The presence of positive feedback is a necessary condition of bistability [11], and it is frequently encountered in networks that control the above processes [12, 13]. The existence of positive feedback is however not a sufficient condition for bistability; the feedback components must also participate in reactions that generate ultrasensitive responses. More precisely formulated, the emergence of bistability requires the following condition: if the feedback loop is opened, the output response f of the resulting open-loop must be a sigmoidal function of the input ω with a logarithmic sensitivity S_ω^f larger than one; in other words, $f(\omega)$ has to be an ultrasensitive response [14, 15]; $S_\omega^f = \partial \ln f(\omega)/\partial \ln \omega$.

This sufficient condition for bistability is satisfied even in the simplest one-gene feedback loop provided the self-activating transcriptional factor (TF) participates in an ultrasensitive reaction. This is the case when the TF binds cooperatively to the promoter of its own gene or the TF forms dimers to be active.

Bistability can function robustly if its parameter range is broad enough. The logarithmic sensitivity can provide clues about the bistable range of a parameter, as evidenced by the positive correlation between cooperativity and the size of the bistable domain in the parameter space [16–18]. S_ω^f is proportional to the degree of cooperativity (Hill-coefficient). With moderately cooperative binding of the TF to DNA, bistability is restricted to a narrow range of TF affinity; this range broadens as cooperativity increases [17].

This intuitive relationship may be blurred for other types of ultrasensitive reactions, including protein homo-dimerization, sequestration and multistep phosphorylation [19–21]. For example, reducing the production rate of a dimeric TF increases sensitivity but also lowers the concentration of the active TF quadratically, and hence the feedback intensity.

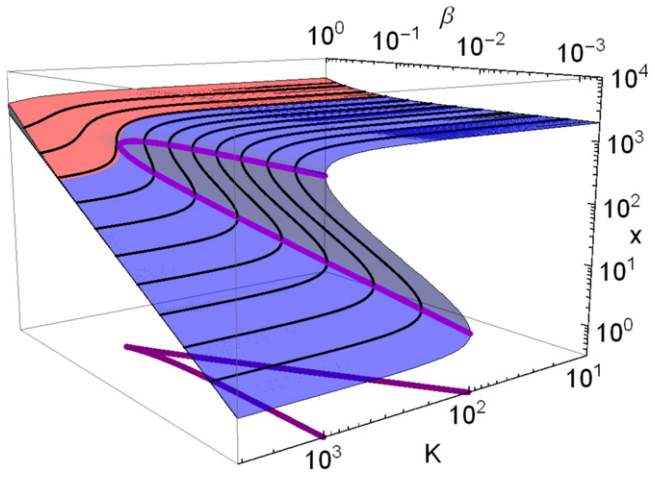

Figure 1. The equilibrium manifold for the simple positive feedback loop with cooperative binding (1), $n = 2$; $V_m = 20$, $\gamma = 0.01$. Fold points (violet) and their projection on the (β, K) plane (dark purple) are indicated. Between the fold bifurcation curves, the system has three equilibria and is bistable. For $\beta > \beta_{\text{cusp}}$, the system is monostable for all values of K and β .

We hypothesized that the trade-off between such effects may maximize the bistable range of a parameter. We sought to identify general conditions for this maximization in a multi-dimensional parameter space. The derived general relations were then tested on prototypical feedback loops incorporating three different ultrasensitive reactions: homo-dimerization, inhibition by sequestration and cooperative binding.

Identifying the maximal bistable range of a parameter permits the robust design of bistable networks and provides answer to the question as to whether bistability is possible in endogenous networks when only the topology and few experimental data are available, which is often the case.

2. Results

2.1. Cusp points delimit the bistable range of two parameters

First, we examined how bifurcation points delimit the bistable range in the parameter space. For this purpose, two key parameters were varied in a simple positive feedback loop with cooperative binding. The system is described by the following equation at equilibrium:

$$\dot{x} = b_P + V_m \frac{x^n}{K^n + x^n} - \gamma x = 0. \qquad (1)$$

The Hill number n is larger than one if the binding is cooperative. γ is the protein degradation rate constant. K is the equilibrium dissociation constant of the TF–DNA binding reaction, and b_P is the basal production rate. The ratio of the basal (b_P) to the maximal (V_m) production rate, $\beta = b_P / V_m$, is a dimensionless parameter and can be used to compare different feedback loops. The inverse of this parameter is the feedback expression (dynamic) range.

Figure 1 illustrates the equilibrium manifold of system (1). For low values of β, the manifold is S-shaped and has two turning points, which represent fold (saddle-node) bifurcation points. The two fold bifurcation points determine the bistability range of K in which system (1) has three distinct equilibria. As β increases, the two fold points move toward each other and collide at a cusp bifurcation point.

Since the intersection of the fold curves is tangential [22], the cusp point defines the maximum of parameter ranges in a two-parameter space in which bistability can occur (figure 2(a), right).

The condition for bistability is defined in terms of logarithmic sensitivity of the open-loop response. Therefore, it is important to see how bifurcations arise in this context (see also appendix A). The intersection of $x = f(\omega)$ with the equivalence line $x = \omega$ determines the number of equilibria and their values. If $f(\omega)$ intersects with the equivalence line tangentially, the system undergoes a fold (saddle-node) bifurcation (figure 2(a), table A1). When β is increased and K is adjusted so that the equivalence line intersects $f(\omega)$ at its inflection point, then these values of β and K define the position of the cusp bifurcation point (figure 2(a)).

2.2. Absence of extrema on the fold-curves

The cusp points represent the extremal values of the bistable domains since the fold curves are monotone with respect to the parameters, i.e. they do not turn back (figures 1 and 2). If the fold-bifurcation curves were not monotone, they might delimit the extrema of bistable parameter domains. To explore this possibility, we defined a general condition for the existence of non-monotone fold curves.

The locus of fold points satisfies $C^{(1)}$ and $C^{(2)}$ in table A1. The fold curve has an extremum in a 2-dimensional parameter space $\{\alpha_i, \alpha_k\}$ if the following expression equals zero,

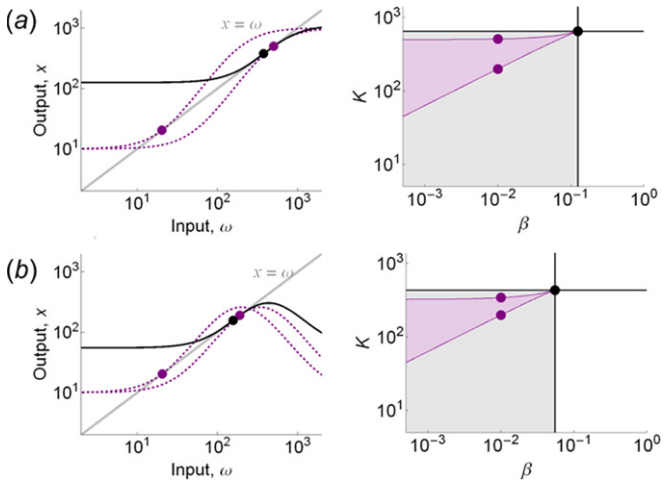

Figure 2. Open loop relations (left) and bistability domains in the parameter space (right) for the feedback loop incorporating the promoter with the sigmoidal (equation (1)) (a) or bell-shaped (equation (17)) (b) response. $n = m = 2$; $V_m = 20$, $\beta = 10^{-2}$ and $\gamma = 0.01$. The correspondence is shown for a pair of fold bifurcation points (purple) and the cusp point (black). The black shaded region defines the parameter domain where bistability is possible while the purple region is the actual bistability domain.

$$\frac{\mathrm{d}\alpha_i}{\mathrm{d}\alpha_k} = -J_{\omega i}^{-1}\frac{\mathrm{d}C}{\mathrm{d}\alpha_k} = -\frac{\det J_{\omega k}}{\det J_{\omega i}} = -\frac{\partial f/\partial\alpha_k}{\partial f/\partial\alpha_i}, \quad (2)$$

where C stands for $C^{(1)}$ and $C^{(2)}$. This is the case if $\partial f/\partial\alpha_k = 0$ provided $\partial f/\partial\alpha_i \neq 0$. Thus, an extremum in the fold curve can arise if the open-loop response is non-monotone with respect to a reaction parameter. Most well-characterized reactions in gene networks display monotone responses to variations in the relevant parameters. An exception may be the bell-shaped response, which is the product of Hill-functions for activation and repression. The bell-shaped response can arise in promoters subject to transcriptional interference or feedforward regulation, and is characterized by a low noise behavior [23, 24]. It has a non-monotone dependence on the state variable (figure 2(b), left). Similarly, $\partial f/\partial K = 0$ for some parameter values because the exchange of ω and K preserves the response function [23]. However, $\partial f/\partial K = 0$ and the fold condition $\partial f/\partial\omega = 1$ cannot be met simultaneously (see appendix B).

Consequently, there is no extremum in the fold curves. In fact, the overall bistability range is very similar to that of the simple cooperative feedback despite the extremum in the bell-shaped response function (figure 2, right).

Thus, the cusp point is generally expected to delimit the range of two parameters, in which bistability is permitted.

2.3. Derivation of general conditions for the existence of extrema in the locus of cusp points

In order to detect the parameters that can maximize the permitted bistable range of another parameter, we set up the following equations, which establish the necessary conditions for the existence of a cusp bifurcation point, upon eliminating three degrees of freedom,

$$\begin{aligned} C^{(1)}(\omega;\,\alpha) &= f(\omega;\,\alpha) - \omega = 0,\\ C^{(2)}(\omega;\,\alpha) &= \frac{\partial f(\omega;\,\alpha)}{\partial\omega} - 1 = 0,\\ C^{(3)}(\omega;\,\alpha) &= \frac{\partial^2 f(\omega;\,\alpha)}{\partial\omega^2} = 0. \end{aligned} \quad (3)$$

Without loss of generality, ω, α_i and α_j have to be expressed in terms of all the remaining parameters $\{\alpha_l\}$ $(l \neq i, j)$.

Importantly, determining the derivatives of α_i or α_j with respect to an arbitrary $\alpha_k \in \{\alpha_l\}$ $(l \neq i, j)$ will permit finding the conditions for an extremal point in the hypersurface of cusp points.

According to the implicit function theorem,

$$\frac{\mathrm{d}\alpha_i}{\mathrm{d}\alpha_k} = -J_{\omega ij}^{-1}\frac{\mathrm{d}C}{\mathrm{d}\alpha_k} = -\frac{\det J_{\omega kj}}{\det J_{\omega ij}}. \quad (4)$$

The Jacobi determinant in the numerator of equation (4) is given as (see also appendix C):

$$\det J_{\omega kj} = \frac{\partial^3 f}{\partial\omega^3}\left(\frac{\partial f}{\partial\alpha_k}\frac{\partial^2 f}{\partial\alpha_j\partial\omega} - \frac{\partial f}{\partial\alpha_j}\frac{\partial^2 f}{\partial\alpha_k\partial\omega}\right). \quad (5)$$

Assuming the genericity condition $\partial^3 f/\partial\omega^3 \neq 0$ is satisfied, a maximum exists if the second factor in (5) is zero. This is equivalent to:

$$S_\omega^{\partial_{\alpha_j} f} - S_\omega^{\partial_{\alpha_k} f} = 0. \quad (6)$$

The choice of parameters for α_j and α_k is made easier by identifying a specific parameter that satisfies $f(\omega;\,\alpha_C) = f(\omega g(\alpha_C);\,1)$. α_C is covariant with the state variable; therefore, we term it covariant parameter, and g is an arbitrary smooth function with non-zero derivative at α_C. It can be shown that $S_\omega^{\partial_{\alpha_C} f} = 1$ at the cusp point (appendix D).

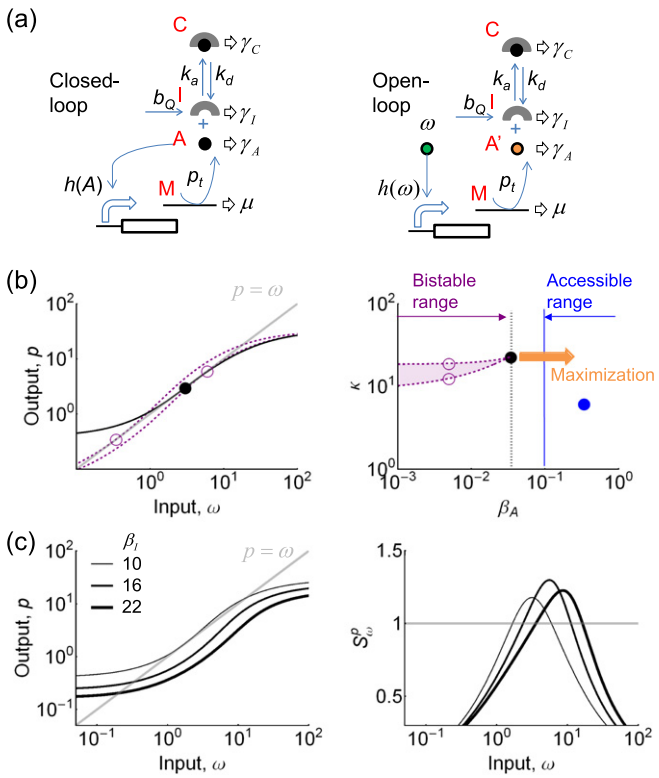

Figure 3. Open and closed loop responses in feedback loop with sequestration. (a) Scheme of reactions in the open-loop (right) upon breaking the closed-loop (left) at the protein A. The decay rate constants of the proteins and mRNA are denoted by γ and μ, respectively. (b) Correspondence of fold (purple) and cusp (black) bifurcation points between the open- (left) and closed-loop system (right). The blue point represents the maximal bistable value of β_A, which lies within the range of the accessible parameter values (hypothetically defined). (c) The dependence of the open-loop response function (left) and its sensitivity (right) on β_I (the other parameters are fixed at $\kappa = 11$, $\chi = 35$, $\beta_A \approx 0.06$).

Now, taking $\alpha_j = \alpha_C$, one can define the possible parameter pairs $\{\alpha_C, \alpha_k\}$ to proceed with in the analysis of a reaction model. Furthermore, one can recognize that,

$$\partial_\alpha S_\omega^f = 0 \Leftrightarrow S_\omega^{\partial_\alpha f} = 1. \tag{7}$$

With (7), it is possible to re-state (6) as

$$\frac{\partial S_\omega^f}{\partial \alpha_C} = 0 \text{ and } \frac{\partial S_\omega^f}{\partial \alpha_k} = 0. \tag{8}$$

This central result establishes a link between local features of the open loop response and bifurcation behavior: the maximum of S_ω^f with respect to two reaction parameters defines the extremum of the bistable range of a third parameter.

A point in the locus of cusp points in the (α_i, α_j) plane that satisfies the double maximum $\{\alpha_j = \alpha_C, \alpha_k\}$ is an extremal value in α_i, provided $\partial_i S_\omega^f - \partial_j S_\omega^f \neq 0$.

A similar statement can be formulated for the other possible pair in the (α_i, α_j) plane: a point that satisfies the double maximum $\{\alpha_k = \alpha_C, \alpha_i\}$ is an extremal value in α_j.

Next, we applied condition (8) to analyze feedback prototypes in different parameter spaces. We always include the parameter pair representing the feedback expression range and binding affinity of the TF to DNA. This facilitates the consistent comparison of the different feedback loops.

2.4. Detection of reaction pairs that maximize bistability in the one-gene loop with sequestration

First, we examined a positive feedback circuit inhibited by sequestration. Sequestration is a common but often hidden source of non-linearity that can significantly alter system behavior, which underscores the importance of this prototype of bistable feedback loops [19, 20, 25]. In this feedback circuit, the TF (A) binds to the promoter and activates the production of its own mRNA (M); A can also be sequestered by an inhibitor (I) into a complex (C), which cannot bind to the promoter (figure 3(a)). The promoter response is described by a Hill-function. The system is described by:

$$\begin{aligned}
\dot{M}(t) &= b_M + V_m \frac{A^n}{K^n + A^n} - \mu M(t),\\
\dot{A}(t) &= p_t M(t) - k_a A(t) I(t) + k_d C(t) - \gamma_A A(t),\\
\dot{I}(t) &= b_Q - k_a A(t) I(t) + k_d C(t) - \gamma_I I(t),\\
\dot{C}(t) &= k_a A(t) I(t) - k_d C(t) - \gamma_C C(t),
\end{aligned} \tag{9}$$

where $b_Q = b_I \frac{p_t}{\mu}$ is the protein production of the inhibitor; k_a and k_d are the protein association and dissociation rate constants, respectively.

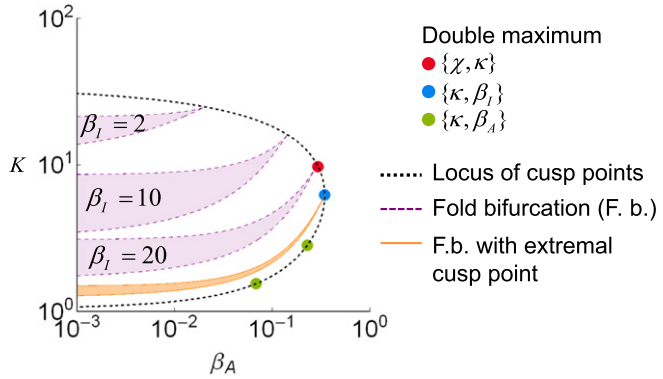

Figure 4. Maximal bistable range for the feedback loop with sequestration, (12) with $n = 1$, $\chi = 35$. β_I was varied (fold curves in purple are shown for illustration). For the extremal value of β_A, $\beta_I(\chi)$ is tuned to 27.18 (30). The orange full lines stand for fold curves that intersect at the cusp point maximized by the indicated parameter pair. The positions of other double maxima are also shown, which are not associated with extrema in this parameter space. A set of realistic parameter values were chosen, $\gamma_C = 0.02\ \text{min}^{-1}$, $\gamma_I = 0.01\ \text{min}^{-1}$, $k_a = 0.1\ \text{nM}^{-1}\ \text{min}^{-1}$, and $k_d = 0.18\ \text{min}^{-1}$, so that $K = \kappa$.

To further simplify the system before opening the loop, it was reduced to two variables and non-dimensionalized:

$$\begin{aligned} \beta_A + \frac{p^n}{\kappa^n + p^n} - m &= 0, \\ \chi m - p - \beta_I \frac{p}{p+1} &= 0. \end{aligned} \tag{10}$$

m and p denote the non-dimensionalized mRNA (M) and monomeric protein (A), respectively.

$$\begin{aligned} \beta_A &= b_M / V_m [1] \\ \chi &= p_t V_m \lambda / \mu \left[s^{-1}\right] \\ \beta_I &= b_Q \lambda \left[s^{-1}\right] \\ \kappa &= K \gamma_A \lambda \left[s^{-1}\right] \\ \text{where } \lambda &= k_a \gamma_C / \gamma_A \gamma_I \left(k_d + \gamma_C\right) \left[M^{-1}\right]. \end{aligned} \tag{11}$$

The SI units are given in brackets. Upon opening, the following equation is obtained:

$$\begin{aligned} \beta_A + \frac{\omega^n}{\kappa^n + \omega^n} - m &= 0, \\ \chi m - p - \beta_I \frac{p}{p+1} &= 0. \end{aligned} \tag{12}$$

This opening corresponds to 'breaking' A into two parts. In the resulting open-loop system, two different components arise from A. The first part serves as the input ω and the sole reaction it imitates is the binding to the promoter. The second part, A' is retained in all the other reactions and becomes the output of the response function (figure 3(a)).

The resulting open-loop response and the bifurcation diagram (figure 3(b)) are similar to that of the simple positive feedback loop (figure 2(a)) when the feedback expression range, β_A^{-1}, and the binding affinity of the TF to the DNA, κ, are varied. On the other hand, the loop with the sequestration has two other parameters and they may have non-trivial impact on system behavior. When β_I, the inhibitor production rate, is increased, the open-loop response is lowered (figure 3(c)). At the same time, the maximal value of S_ω^p displays a non-monotone response, pointing to the possibility that there is an optimal value of β_I that maximizes the bistable range of β_A.

For the above opening (12), the covariant parameter is κ. Thus, $g(\kappa) = 1/\kappa$. Applying the conditions for the double maxima, $C^{(1)}$, $C^{(2)}$ and equation (8), to the response function constructed from equation (12) reveals that all three possible pairs of parameter combinations of κ have joint maxima.

- $\{\chi, \kappa\}$ has the most permissive conditions: $n \geqslant 1$, $\beta_I > 0$, $\beta_M > (n-1)^2/4n$.
- $\{\kappa, \beta_I\}$ double maximum exists if $\beta_I > 1$, $n \geqslant 1$.
- $\{\kappa, \beta_A\}$ exists only if $\beta_I > 27$ (or $\chi > 32$), $n \geqslant 1$.

In order to focus on sequestration, no cooperativity was included in the analysis, $n = 1$. Thus, sequestration was the sole source of ultrasensitivity.

The four reduced parameters contain multiple reaction parameters that often belong to consecutive or related reactions and therefore, they describe a specific property, exemplified by the feedback expression range, β_A^{-1}. When a reduced parameter contains unrelated reaction parameters, as well, it is possible to focus on a dominant or unique reaction parameter by varying it, while keeping the others fixed. In this way, χ reflects the maximal production rate of the transcriptional activator; κ reflects the TF–DNA binding affinity and β_I the inhibitor production rate.

For the (β_A, κ) plot when β_I is varied, the relevant double maximum is $\{\kappa, \beta_I\}$. The optimal inhibitor production rate that maximizes the bistable range of β_A is $\beta_I = 27.18$ when $\chi = 35$ (figure 4), revealing that the maximal bistable feedback expression range is attained when the inhibitor production rate nearly reaches the level of the maximal activator production

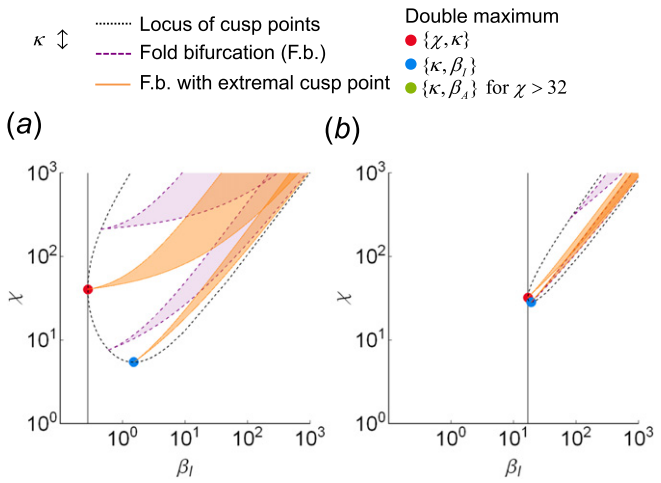

Figure 5. Maximal bistable ranges for the feedback loop with sequestration at broad and narrow feedback expression ranges (β_A^{-1}); $n = 1$ (12); κ was varied (purple curves): $\kappa = 5$ (bottom), 200 (top). (a) $\beta_A = 10^{-3}$. $\kappa \approx 2.8$ for $\{\kappa, \beta_I\}$ and $\kappa \approx 11.8$ for $\{\kappa, \chi\}$. The extremal value (black line) of β_I is 0.28. (b) $\beta_A = 1/4$. The extremal value (black line) of β_I is 16.9.

rate. To visualize the maximal bistable range, we plotted the locus of cusp points as β_I was varied (figure 4).

The extremal value of β_A for the $\{\kappa, \beta_I\}$ double maximum can be conveniently expressed as a function of χ (31) or β_I (13).

$$\beta_A|_{\{\kappa,\beta_I\}} = \frac{\left(\sqrt{\beta_I} - 1\right)^3}{8\beta_I}. \qquad (13)$$

For the above example, $\beta_A = 0.34$ (figure 4). The fact that β_A^{-1} typically ranges from 10 to 1000 in networks with multiple feedback loops [26] reveals that bistability is possible even with very narrow feedback expression range, $\beta_A^{-1} \approx 3$.

The equation (13) also reveals that β_A increases with β_I.

Interestingly, there are two relevant double maxima in the (β_I, χ) plane, when κ is varied (figure 5): $\{\kappa, \beta_I\}$defines the extremum in χ, while the $\{\chi, \kappa\}$ pair defines the extremum in β_I.

It is interesting to explore how realistic values of β_I can promote bistability (appendix E). We explored two limiting scenarios with respect to the feedback expression range, β_A^{-1}. For this purpose, β_I was expressed in terms of β_A.

$$\beta_I|_{\{\chi,\kappa\}} = 8\Big(3\beta_A + 4{\beta_A}^2 + \sqrt{\beta_A + 9{\beta_A}^2 + 24{\beta_A}^3 + 16{\beta_A}^4}\Big). \qquad (14)$$

If β_A^{-1} is large, then bistability is possible with very low inhibitor production rate or affinity. For example, for $\beta_A = 10^{-3}$, $\beta_I = 0.28$ using (14). Since β_I contains parameters for the rate of production of the inhibitor and for its binding to the activator, the following combinations were considered.

If transcription rate is low (table E1), then $\lambda = 0.28\ \mathrm{min}^{-1}$ (appendix F). Consequently, the inhibitor affinity, $K_{\mathrm{inh}} = k_d/k_a$, has to be less than 350 nM for bistability to emerge (figure 5(a)). On the other hand, when transcription rate is high even a very weak binding ($K_{\mathrm{inh}} = 35$ mM) is sufficient to support bistability. This points to the possibility that a highly expressed inhibitor protein can generate bistability even if the binding is weak, potentially representing non-specific protein–protein interaction, which may be overlooked in standard experimental conditions.

Is bistability possible if the feedback expression range is narrow, e.g. $\beta_A^{-1} = 4$? For $\beta_A = 1/4$, $\beta_I = 16.9\ \mathrm{min}^{-1}$ (14), (figure 5(b)). Assuming weak and strong transcription rates, 5.8 and 590 nM inhibitor affinities are needed, respectively, to generate bistability. This indicates that bistability can emerge in the range of typical protein binding constants even with a narrow, fourfold, dynamic range of feedback expression.

2.5. Analysis of the one-gene loop with protein homo-dimerization

Next, we examined if maxima exist in the locus of cusp points for a one-gene model with protein homo-dimerization (figure 6). The TF binds to the promoter only as dimer C. To focus on the effect of homodimerization, the dimer binds to the promoter non-cooperatively. The system was non-dimensionalized and then opened (appendix G). The main reduced parameters are dominated by the following reactions: χ by the maximal rate of activator production, κ_q by the binding strength in the homodimerization, and κ_d by the TF–DNA affinity. β^{-1} is the feedback expression range. The covariant parameter is κ_d.

No positive real (physical) solution was found for any of the possible parameter pairs $\{\kappa_d, \alpha_k\}$ that satisfies the conditions for the cusp points and equation (8). Thus, the cusp points delimiting the bistability domains lack extrema for positive parameter values.

This can be illustrated by varying the dissociation rate of the dimer into the monomer (figure 6). At

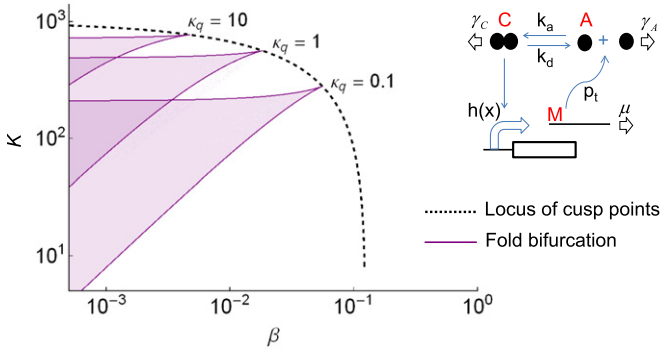

Figure 6. Monotonically increasing bistable expression range as dimerization strength, κ_q is lowered $\chi = 20$, $n = 1$, $V_m = 1$. $\kappa_q(k_d)$ is indicated for each pair of fold bifurcation curves ($k_d \approx 2$, 20 and 200 min^{-1} from top to bottom). K was expressed from κ_d so that, $\gamma_A = \gamma_C = 0.01\ \text{min}^{-1}$, $k_a = 0.1\ \text{nM}^{-1}\ \text{min}^{-1}$.

strong dimerization ($\kappa_q = 10$, the dimerization equilibrium constant $K_{\text{dim}} = k_d/k_a \approx 20$ nM), the bistability domain is small. This is because the TF concentration has to be below K_{dim} to have sufficiently high logarithmic sensitivity in the open-loop response. Since the concentration of the TF is around 2000 nM in the higher stable equilibrium, the ultrasensitivity necessary for bistability is possible only if the basal expression is around 100 times less than the maximal expression, resulting in concentrations of around 20 nM (figure 6). Indeed, bistability appears only when $\beta < 10^{-2}$. The TF–DNA binding affinity is low (higher than 200 nM) in this bistable domain.

A reduction of the dimerization expands the bistable range of β (figure 6). Above $K_{\text{dim}} \approx 2000$ nM (i.e. below$\kappa_q = 0.1$), the expansion of the bistable range levels off. Indeed, if κ_q is set to zero by eliminating the dimer decay, β approaches 1/8, which is the same value as the positive feedback loop with a cooperative promoter, $n = 2$ (appendix G.2).

Thus, in this range of low dimerization strengths (high K_{dim}, low κ_q), a further weakening of dimerization does not increase ultrasensitivity and the lower dimer concentration is compensated by the stronger binding of the TF to DNA. This explains the absence of maximum in the locus of cusp points. Having no optimal value for the dimerization binding, the feedback loop can generate a robust bistability in the face of variations in K_{dim}.

2.6. Optimal parameter values for the broadest bistable parameter range in the two-gene loop with mutual activation

Next, we examined a feedback loop enclosed by two transcriptional activators. The cooperative binding of the transcriptional activator to the promoter provides the source of ultrasensitivity. The system dynamics is defined by the feedback expression ranges (β_1^{-1}, β_2^{-1}) and the binding strengths of the two transcriptional activators to the DNA (κ_1, κ_2) (figure 7).

Despite the simple reaction scheme and the simple form of ultrasensitivity, two double maxima were identified (appendix H), revealing that with cooperativity as sole source of ultrasensitivity, nonmonotone parameter domains can arise.

The {κ_1, κ_2} double maximum exists under permissive conditions and defines the extremum in β_1 as κ_2 is varied in the (β_1, κ_1) plane.

In order to assess how the affinities affect the bistability range we explored the relationship between κ_1 and κ_2 at the cusp points. There is an inverse relation between κ_1 and κ_2 in the bistable domains. At $\kappa_1 = 5$, the bistable domain is narrow (figure 7(a)). As κ_1 is decreased, κ_2 increases and the bistable range of β_1 expands. At the extremum in β_1, the two affinities have similar values (figure 7(a)).

To assess the above relation more quantitatively, symmetric conditions were enforced in the reaction scheme. The Hill coefficients were set equal. Secondly, β_1 and β_2 were required to be equal at the extremum of the cusp points (47). With these two constraints, the two affinities were indeed equal at the maximal point (48). This confirms that the broadest bistable range in β_1 and β_2 is attained when the affinities are equal. It also hints to why the values of κ_1 and κ_2 are similar even when the two basal production rates are different.

It is interesting to observe that the bistability range of β_1 declines very rapidly when κ_1 increases beyond the optimal value (figure 7(a)). This behavior is even more pronounced when the Hill coefficient assumes larger values. In this case, a new extremum arises, which delimits κ_1 at low affinities. Thus, the extremum is surrounded by very asymmetric range of κ_1 values in which bistable domains arise (figure 7(b)).

The extrema in this feedback loop can be compared to those with other forms of binding reactions. In both homo- and heterodimerization two proteins interact. Thus, cooperative binding to two sites in the promoter permits a consistent comparison. If the cooperativity of the binding to the two sites is large then the Hill coefficient, $n = 2$ [27]. For $n = 2$, the extremal values in the normalized basal expression is 1/8 (49), which is the same as the limiting value in homodimerization but less than 1/3, the value found for the loop with sequestration with realistic parameters (13).

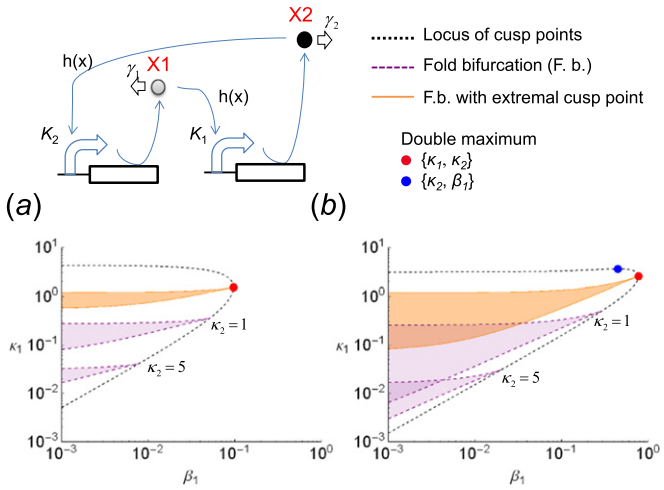

Figure 7. Extrema of the bistability domain for the feedback loop with mutual activation. $\beta_2 = 0.01$. κ_2 was varied. (a) $m = n = 1.5$. The extremal value of β_1 is 0.096 (at $\kappa_2 \approx 0.23$). (b) $m = 3$, $n = 2$. The extremal value of β_1 is 0.78 (at $\kappa_2 \approx 0.12$).

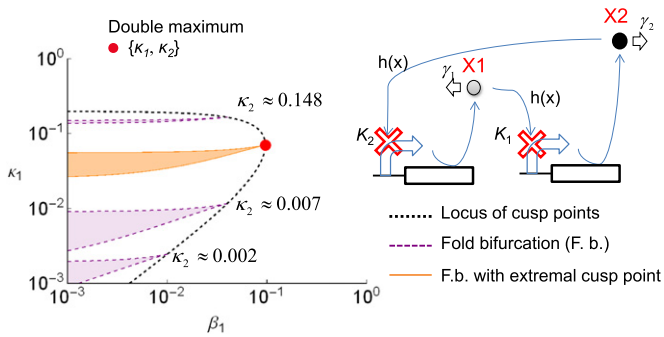

Figure 8. Maximal bistable range for the basal expression β_1 in the toggle-switch. $m = n = 1.5$ and $\beta_2 = 0.01$. κ_2 was varied. For the bistable regions (purple) the values of $\kappa_2$were selected to have $\beta_1 = 0.01$ and 0.04 at the cusp point. The extremal value of β_1 is 0.096 (at $\kappa_2 \approx 0.12$).

2.7. Optimal parameter values for the broadest bistable parameter range in the two-gene loop with mutual repression

Positive feedback can be also realized by two mutually inhibiting repressors, also known as the toggle-switch [16].

The locus of cusp points reveals a behavior similar to that of the two-gene loop with activators (appendix I, figure (8)). The main difference is that in this case the affinities of the two transcriptional factors are similar in all the bistable domains. Weak binding affinity of one repressor entails weak binding affinity of the other repressor in the bistable domains.

3. Discussion

3.1. Maximizing sensitivity with respect to two parameters maximizes the bistable range of a third parameter

The logarithmic sensitivity provides a practical tool to predict and analyze bistability. Sensitivity can be easily obtained from the open-loop response fitted to experimental data.

Maximizing sensitivity was shown to specify the broadest dynamic range of a single parameter in a simple positive feedback loop with cooperative binding [17], similar to figure (1). When such an approach was applied for more complex feedback loops, a high statistical correlation was seen between the maximal sensitivity and bistability range [28]. It has remained unclear how to formulate a condition so that the correlation becomes full (i.e. one) and what analytical relations can be obtained for that.

In this work, we derived a general rule that stipulates that the largest bistable range of a parameter, i.e. extremum of a bistable domain, (equation (8)), is attained when the sensitivity of the response function has a maximum against two other parameters. We then verified whether such parameter pairs were present in specific network topologies, by obtaining analytical relations (e.g. equation (13)). This allows drawing general conclusions on specific network topologies since the entire parameter space was captured. These relations revealed that the prototypical feedback enclosed by protein dimers has no such

reaction pairs. Conversely, loops with sequestration and two-gene loops with cooperative binding do have such reaction pairs despite the distinct nature of the sequestration and cooperative binding to DNA. Also, loops having similar reactions, such as homo- and heterodimerization, (sequestration) fall in distinct categories with respect to the existence of maxima in bistable regions.

This suggests that not the chemical-kinetic nature of a specific reaction but the interaction of all reactions determines whether or not such parameter pairs are elicited. Most complex networks that display bistability are derivatives of a few prototypical network topologies and reactions [28–32]. It will be interesting to explore how the number of maximizing reaction parameter pairs varies as the complexity of a network increases.

3.2. Maximizing bistability and the design of bistable networks

In order to design a bistable gene network, an ultrasensitive reaction must be included. Furthermore, the system parameters have to assume values within the bistable parameter range. If the accessible parameter range does not overlap with the bistable range one can alter the reaction parameter physically or biologically to broaden the accessible range (figure (3)). However, there are often limits to how much the accessible range can be widened. For example, the feedback expression range is often delimited by the lowest possible value of basal transcription rate, also known as leakage (figure 1(b)) [26]. In some promoters, the basal expression has counter-intuitive determinants. For example, if the number of activator binding sites is reduced in the promoter the leakage increases despite the fact that the maximal expression is reduced [26]. In this case it is very difficult to broaden the range of the feedback expression.

If it is not possible to enlarge the accessible range of a reaction parameter in the cells, one alternative is to expand the bistable range. Our results provide support for this possibility: the bistable range of a parameter can be expanded by tuning other parameters to enable the emergence of bistability. Even if the range of particular parameter in a system is severely constrained, many others may be broadly tuned.

The conditions we derived in this work identify the pairs of parameters that maximize the bistable range of a parameter under consideration (8). For example, knowing the affinity of the inhibitor to the TF and the maximal transcription rate of the positive feedback loop permits the calculation of the optimal inhibitor production rate. Tuning this parameter to its optimal value makes it possible for bistability to occur even if the feedback expression range is very narrow (figure 5). When the parameter is tuned away from this optimal value the bistable feedback expression range shrinks rapidly.

In contrast, the loop with homodimerization does not have optimal values, and the bistable feedback expression range remains relatively constant and close to the limiting value as soon as sufficiently weak dimerization strength is reached (figure 6). This indicates that bistable feedback expression range of the loop with homodimerization is not highly sensitive to variations in the dimerization strength, reflecting the absence of double maxima, which typically makes the bistable ranges sensitive to parameter variations.

In the two-gene loops with cooperative binding, the two TFs must have similar or equal affinities to maximize the bistable feedback expression range. For the mutual repression loop, the affinities are similar also in other bistable domains, where the affinities are not optimal (figure 8). Interestingly, the opposite relation is observed in loop with mutual activation. The further away the value of an affinity is shifted from the optimal value, the more different the affinities of the two TF have to be to generate bistability (figure 7).

3.3. Detection of bistability in endogenous networks

Endogenous bistable networks are subject to constraints similar to that encountered in the design of the networks. Further constraints arise during evolution when a reaction controls different biological functions or a single function in different environments with conflicting demands on the reaction parameters [33–35].

Our results may shed light on the prevalence of the different types of feedback loops. Interestingly, the mutually activating and repressing loops have identical maximal bistable feedback expression ranges (figures 7 and 8). That may explain why both network topologies have been identified in the model organism budding yeast [29].

The conditions for the extremal points also help to assess whether bistability is possible in endogenous networks when few data are available, which is typically the case. Most of the time, the network topology is identified and gene expression data can be easily measured, which can also define feedback expression range. For this reason, we compared the extremal value of the feedback expression range in prototypical feedback loops. Interestingly, heterodimerization (sequestration) outperforms both cooperativity and homodimerization since only sequestration permits the occurrence of bistability if the feedback expression range is less than eight.

Moreover, our results suggest that unexplained bistability may arise in positive feedback loops with no obvious ultrasensitive reaction because even very weak, and hence unidentified, interaction with inhibitors can generate bistability by sequestration.

Determining the limits of bistability in networks is particularly important in networks that control cellular differentiation [36].

Acknowledgments

This work was supported by the Swiss National Science Foundation (SNSF). We thank F Maleki, for

Table A1. Conditions for fold ($C^{(1)}$ and $C^{(2)}$) and cusp ($C^{(1)}$, $C^{(2)}$ and $C^{(3)}$) bifurcations. The brackets denote the inner product.

	Multi-dimensional[a]	One-dimensional with $f(\omega;\alpha)$	Sensitivity of open-loop response S_ω^f
$C^{(1)}$: equilibrium	$F(x;\alpha)=0$	$f(\omega)=\omega$	—
$C^{(2)}$: fold	$J\cdot q=0$: $\det J=0$	$\partial_\omega f=1$	$S_\omega^f=1$
$C^{(3)}$: cusp	$\langle\tilde{q},\langle q, H\cdot q\rangle\rangle=0$	$\partial_{\omega\omega} f=0$	$\partial_\omega S_\omega^f=0$

[a] J is the Jacobian matrix: $J_{ij}=\partial F^{(i)}/\partial x_j$. q is the null eigenvector of the Jacobian matrix, $J\cdot q=0$ so that it is normed to one, $<q, q>=1$. H is the Hessian matrix, $H_{kl}^{(i)}=\partial^2 F^{(i)}/\partial x_k \partial x_l$, and $\tilde{q}$ is the adjoint null eigenvector of the Jacobian matrix, $\tilde{q}\cdot J=0$, that is $J^T\cdot\tilde{q}=0$; $<q,\tilde{q}>=1$.

helpful discussions and O Hallatschek, A Denz and A de los Reyes V for comments on the manuscript.

Appendix A. Relation between the bifurcation conditions formulated for the closed- and open-loop systems

The closed-loop formulation $F(x;\alpha)$ is converted to the following one-dimensional expression:

$$F(x;\alpha)=f(x;\alpha)-x=0. \tag{15}$$

The open-loop response function $f(\omega;\alpha)$ is then given by replacing x in $f(x;\alpha)$ with ω:

$$\eta=x=f(\omega;\alpha). \tag{16}$$

It is clear that the equilibrium condition $C^{(1)}$ for the open-loop re-closes the loop.

The bifurcation conditions for the multidimensional closed-loop system [22] are also given in table A1.

Appendix B. Fold points for the feedback loop with the bell-shaped response

The positive feedback incorporating a promoter with the bell-shaped response is described at equilibrium by

$$b_P+V_m\frac{x^n}{K^n+x^n}\frac{K^m}{K^m+x^m}-\gamma x=0. \tag{17}$$

Thus, the open-loop response function is given by

$$x=f(\omega)=\frac{1}{\gamma}\left(b_P+V_m\frac{\omega^n}{K^n+\omega^n}\frac{K^m}{K^m+\omega^m}\right). \tag{18}$$

The bell-shaped response is the product of Hill-functions for an activator and a repressor. It can be seen that the exchange of K and ω does not change the equation and the response function has maxima with respect to both K and ω.

The fold condition and $\partial f/\partial K=0$ have to be satisfied simultaneously for the fold curve to display a maximum:

$$\frac{\partial f}{\partial\omega}=\left(\left(K^{m-1}\omega^n\left(nK^{m+n}+K^n(n-m)\omega^m-m\omega^{m+n}\right)\Big/\left(\gamma\left(K^m+\omega^m\right)^2\times\left(K^n+\omega^n\right)^2\right)\right)=1, \tag{19}$$

$$\frac{\partial f}{\partial K}=-\left(\left(K^m\omega^{n-1}\left(nK^{m+n}+K^n(n-m)\omega^m-m\omega^{m+n}\right)\Big/\left(\gamma\left(K^m+\omega^m\right)^2\times\left(K^n+\omega^n\right)^2\right)\right)=0. \tag{20}$$

However, the two conditions are contradictory. Therefore, there are no extrema on the fold curves.

Appendix C. Calculation of the Jacobi determinant for the hypersurface of the cusp points

$$\det J_{\omega kj}=\begin{vmatrix}\frac{\partial C^{(1)}}{\partial\omega}&\frac{\partial C^{(1)}}{\partial\alpha_k}&\frac{\partial C^{(1)}}{\partial\alpha_j}\\ \frac{\partial C^{(2)}}{\partial\omega}&\frac{\partial C^{(2)}}{\partial\alpha_k}&\frac{\partial C^{(2)}}{\partial\alpha_j}\\ \frac{\partial C^{(3)}}{\partial\omega}&\frac{\partial C^{(3)}}{\partial\alpha_k}&\frac{\partial C^{(3)}}{\partial\alpha_j}\end{vmatrix}=\begin{vmatrix}0&\frac{\partial f}{\partial\alpha_k}&\frac{\partial f}{\partial\alpha_j}\\ 0&\frac{\partial^2 f}{\partial\alpha_k\partial\omega}&\frac{\partial^2 f}{\partial\alpha_j\partial\omega}\\ \frac{\partial^3 f}{\partial\omega^3}&\frac{\partial^3 f}{\partial\alpha_k\partial\omega^2}&\frac{\partial^3 f}{\partial\alpha_j\partial\omega^2}\end{vmatrix}=\frac{\partial^3 f}{\partial\omega^3}\left(\frac{\partial f}{\partial\alpha_k}\frac{\partial^2 f}{\partial\alpha_j\partial\omega}-\frac{\partial f}{\partial\alpha_j}\frac{\partial^2 f}{\partial\alpha_k\partial\omega}\right). \tag{21}$$

Table E1. The range of realistic transcription rates and the resulting RNA and protein concentrations. For proteins nuclear localization was assumed.

Production rate	p_R (RNA)/p_P (protein) (nM min^{-1})	RNA (copy/cell)	Protein (copy number/cell)/(nM)
Low	0.005/1	0.1	200/100
High	0.5/100	10	20 000/10 000

Appendix D. S_ω^f as a function of the covariant parameter

If there exists a parameter α_c for which the response function can be re-written as

$$f(\omega;\alpha_C) = f\Big(\omega g(\alpha_C);1\Big), \tag{22}$$

so that $g(\alpha_c) \neq 0$ and $g'(\alpha_c) \neq 0$, then $S_\omega^{\partial_{\alpha_C} f} = 1$ at the cusp point. The proof can be seen by applying constraints $C^{(1)}$, $C^{(2)}$ and $C^{(3)}$ to equation (22):

$$\frac{\partial f}{\partial \omega} = f'\Big(\omega g(\alpha_C)\Big) g(\alpha_C), \tag{23}$$

$$\frac{\partial f}{\partial \alpha_C} = f'\Big(\omega g(\alpha_C)\Big) \omega g'(\alpha_C), \tag{24}$$

$$\frac{\partial^2 f}{\partial \omega^2} = f''\Big(\omega g(\alpha_C)\Big) g^2(\alpha_C) = 0, \tag{25}$$

$$\frac{\partial^2 f}{\partial \alpha_C \partial \omega} = f''\Big(\omega g(\alpha_C)\Big) \omega g'(\alpha_C) g(\alpha_C) + f'\Big(\omega g(\alpha_C)\Big) g'(\alpha_C). \tag{26}$$

Then the sensitivity of the α_c—derivative of the response function is

$$\begin{aligned} S_\omega^{\partial_{\alpha_C} f} &= \frac{\omega}{\dfrac{\partial f}{\partial \alpha_C}} \frac{\partial^2 f}{\partial \alpha_C \partial \omega} \\ &= \Bigg(\Big(\omega \Big[f''\Big(\omega g(\alpha_C)\Big) \omega g'(\alpha_C) g(\alpha_C) \\ &\quad + f'\Big(\omega g(\alpha_C)\Big) g'(\alpha_C) \Big] \Big) \Big/ f'\Big(\omega g(\alpha_C)\Big) \\ &\quad \times \omega g'(\alpha_C) \Big) \Bigg). \end{aligned} \tag{27}$$

Applying (25) to (27) yields

$$S_\omega^{\partial_{\alpha_C} f} = 1. \tag{28}$$

Appendix E. Biologically relevant ranges of parameter values

Specific model parameters were representative of reactions in yeast and they fall into a realistic range of values, as detailed below.

The typical yeast mRNA half-lives range between 1 and 10 min (decay rate constant, $\mu = 0.07$–0.7 min^{-1}) [26, 37]. The average protein half-life is 120 min but the half-life of some regulators is shorter by an order of magnitude [38], which results in typical decay rate constants of $\mu = 0.006$–0.06 min^{-1}.

The translation rate p_t ranges from 6 to 20 min^{-1} [39].

Most transcriptional factors and their regulators have mean concentrations between 200 and 2000 molecules/cell [40]. For nuclear proteins, this corresponds to 100–1000 nM, assuming a nuclear volume of 2 μm^3 [37]. Based on these data, the typical RNA production (transcription rate, p_R) and the lumped protein production rates (translation rate, p_P) can be calculated (see table E1).

The relation between p_R and p_P is given by

$$p_P = p_R \frac{p_t}{\mu} = [RNA] \cdot p_t. \tag{29}$$

The equilibrium dissociation constant of proteins ranges between 0.1 and 1000 nM [20]. The typical association rate of proteins is around $k_a = 1.66 \times 10^6$ M^{-1} s^{-1} $= 0.1$ nM^{-1} min^{-1} [41].

Appendix F. Double maxima for the positive feedback with sequestration

When $n = 1$, the following expressions are obtained

$$\beta_I|_{\{\kappa,\beta_I\}} = \frac{1}{128}\Big(16\chi + \chi^2 + \chi^{3/2}\sqrt{32+\chi}\Big), \tag{30}$$

$$\beta_A|_{\{\kappa,\beta_I\}} = \frac{\Big(\sqrt{2}\sqrt{\chi\Big(16+\chi+\sqrt{\chi}\sqrt{32+\chi}\Big)} - 16\Big)^3}{256\chi\Big(16+\chi+\sqrt{\chi}\sqrt{32+\chi}\Big)}. \tag{31}$$

To consider realistic values of physical parameters, we calculated a combination of b_I and $K_{\text{inh}} = k_d/k_a$ for each value of β_I from (32),

$$\beta_I = b_I \lambda = b_I k_a \gamma_C \Big/ \gamma_A \gamma_I \Big(k_d + \gamma_C\Big). \tag{32}$$

For the protein production rate b_I, two different fixed values were used (table E1). For example, if $\beta_I = 16.9$ min^{-1}, then $\lambda = 0.169$ nM^{-1} with the high production rate (table E1), $b_I = 100$ nM min^{-1} (32). With $\gamma_A = \gamma_I = 0.01$ min^{-1} and $k_a = 0.1$ nM^{-1} min^{-1}, this value of λ yields $k_d = 59$ nM min^{-1}. Thus, $K_{\text{inh}} = 590$ nM.

Appendix G. Positive feedback with homo-dimerization

G.1. Reaction scheme and opening

The following equations were used for the reaction scheme in (figure 6):

$$\begin{aligned}\dot{M}(t) &= b + V_m\frac{C(t)^n}{K^n + C(t)^n} - \mu M(t),\\ \dot{A}(t) &= p_t M(t) - 2k_a A(t)^2 + 2k_d C(t) - \gamma_A A(t),\\ \dot{C}(t) &= k_a A(t)^2 - k_d C(t) - \gamma_C C(t).\end{aligned} \tag{33}$$

After non-dimensionalization equation (33) are reduced to:

$$\begin{aligned}\beta + \frac{p^{2n}}{{\kappa_d}^{2n} + p^{2n}} - m &= 0,\\ \chi m - p - \kappa_q p^2 &= 0,\end{aligned} \tag{34}$$

where m and p denote the non-dimensionalized mRNA (M) and monomeric protein (A), respectively, with the following parameters:

$$\begin{aligned}\chi &= p_t V_m/\mu,\\ \kappa_q &= 2\gamma_C k_a/{\gamma_A}^2\left(k_d + \gamma_C\right),\\ \beta &= b/V_m,\\ \kappa_d^2 &= K{\gamma_A}^2\left(k_d + \gamma_C\right)\big/k_a.\end{aligned} \tag{35}$$

The covariant parameter is κ_d.

The loop was opened at the promoter:

$$\begin{aligned}\beta + \frac{\omega^{2n}}{{\kappa_d}^{2n} + \omega^{2n}} - m &= 0,\\ \chi m - p - \kappa_q p^2 &= 0.\end{aligned} \tag{36}$$

G.2. Limiting value of the cusp points

To find the limiting value of basal expression at the cusp point as κ_q declines, κ_q was equated to zero. Non-cooperative binding, $n = 1$, was taken for simplicity. Equation (34) then reduces to:

$$\beta + \frac{p^2}{{\kappa_d}^2 + p^2} - \frac{1}{\chi}p = 0. \tag{37}$$

The above equation is essentially identical to the simple positive feedback loop with a Hill coefficient of 2. Applying the conditions for the cusp bifurcation yields $\beta = 1/8$.

Appendix H. Two-gene loop with activators

H.1. Reaction scheme and opening

The following system equation describes the system:

$$\begin{aligned}\dot{X}_1(t) &= b_1 + V_1\frac{X_2(t)^n}{K_2^n + X_2(t)^n} - \gamma_1 X_1(t),\\ \dot{X}_2(t) &= b_2 + V_2\frac{X_1(t)^m}{K_1^m + X_1(t)^m} - \gamma_2 X_2(t).\end{aligned} \tag{38}$$

The system at equilibrium was non-dimensionalized to:

$$\begin{aligned}\beta_1 + \frac{x_2^n}{x_2^n + \kappa_2^n} - x_1 &= 0,\\ \beta_2 + \frac{x_1^m}{x_1^m + \kappa_1^m} - x_2 &= 0,\end{aligned} \tag{39}$$

with the following parameters:

$$\begin{aligned}\kappa_1 &= \gamma_1\frac{K_1}{V_1}, \quad \kappa_2 = \gamma_2\frac{K_2}{V_2},\\ \beta_1 &= \frac{b_1}{V_1}, \quad \beta_2 = \frac{b_2}{V_2}.\end{aligned} \tag{40}$$

The loop was opened at the promoter:

$$\begin{aligned}\beta_1 + \frac{\omega^n}{\omega^n + \kappa_2^n} - x_1 &= 0,\\ = \beta_2 + \frac{x_1^m}{x_1^m + \kappa_1^m} - x_20.\end{aligned} \tag{41}$$

H.2. Double maxima

The $\{\kappa_1, \kappa_2\}$ double maximum exists for $0 < \beta_1 < \frac{(mn-1)^2}{4m}$ and $0 < \beta_2 < \frac{(m^2n^2-1)^2}{4m^2n^2}$.

Parameters are expressed as a function of β_1 at this point:

$$\begin{aligned}\beta_2|_{\{\kappa_1,\kappa_2\}} = \Bigg(\Bigg(2\sqrt{\beta_1\left(\beta_1+1\right)}\left(1 - m^2n^2\right) + 2\beta_1\\ \left(m^2n^2+1\right) + (mn-1)^2\Bigg)/(4\,mn)\Bigg),\end{aligned} \tag{42}$$

$$\begin{aligned}\kappa_1|_{\{\kappa_1,\kappa_2\}} = \sqrt{\beta_1\left(\beta_1+1\right)}\\ \times\left(\frac{mn\left(4\sqrt{\beta_1(\beta_1+1)} + mn\right) - 1}{mn\left(-4\beta_1 + mn - 2\right) + 1}\right)^{1/m},\end{aligned} \tag{43}$$

$$\begin{aligned}\kappa_2|_{\{\kappa_2,\kappa_2\}} = \left(\frac{\beta_1}{\beta_1+1}\right)^{-\frac{1}{2n}}\cdot\Bigg(\Bigg(2\beta_1\left(m^2n^2-1\right)\\ + \left(1-2\sqrt{\beta_1\left(\beta_1+1\right)}\right)\left(m^2n^2+1\right) - 2\Bigg)\\ /(4\,mn)\Bigg).\end{aligned} \tag{44}$$

The $\{\kappa_2, \beta_1\}$ double maximum exists for

$$\begin{aligned}0 < \beta_1 &< \frac{mn - n - 2}{4},\\ 0 < \beta_2 &< \frac{\left(m^2-1\right)^2n^2 - 4\,mn + 4}{8\,mn}.\end{aligned} \tag{45}$$

Parameters at the extremal points can be expressed analytically:

$$\kappa_2|_{\{\kappa_2,\beta_1\}} = \frac{\sqrt{4\beta_2\left(\beta_2+1\right)m^2+1} - 1}{2\,m}. \tag{46}$$

To examine how the two TF–DNA binding affinities relate to each other at the extrema of cusp points

in the β_1 direction, their relation was examined in symmetric parameter conditions. First the Hill numbers were equated: $m = n = q$. Then, $\beta_1 = \beta_2 = \beta$ and the equation (42) was solved for β:

$$\beta_S = \frac{(q-1)^2}{4q}. \tag{47}$$

This value was then substituted into equations (43) and (44). As a result, the same expressions were obtained for the two affinities (κ_1, κ_2):

$$\kappa_1 = \kappa_2 = \frac{\left(\frac{q-1}{q+1}\right)^{-1/q}\left(q^2-1\right)}{4q}. \tag{48}$$

If the basal expression $\beta_1 = 0$, then (42) becomes

$$\beta_2 = \frac{(mn-1)^2}{4\,mn}. \tag{49}$$

If $m = 1$ and $n = 2$ or $m = n = \sqrt{2}$ then $\beta_2 = 1/8$.

Appendix I. The two-gene loop with repressors

$$\begin{aligned}\dot{X}_1(t) &= b_1 + V_1\frac{K_2^n}{K_2^n + X_2(t)^n} - \gamma_1 X_1(t),\\ \dot{X}_2(t) &= b_2 + V_2\frac{K_1^m}{K_1^m + X_1(t)^m} - \gamma_2 X_2(t).\end{aligned} \tag{50}$$

The non-dimensionalization and opening was performed in the same way as for the two-gene loop with activators (appendix H).

The covariant parameter is κ_2. The $\{\kappa_1, \kappa_2\}$ double maximum exists for $\beta_2 > 0$. A second double maximum $\{\beta_1, \kappa_2\}$ exists for restrictive conditions: $n\left(m + 2\beta_2 - \sqrt{1 + 4\beta_2 m^2(1+\beta_2)}\right) > 2$.

References

[1] Pisarchik A N and Feudel U 2014 Control of multistability *Phys. Rep.* **540** 167–218

[2] Roberts J A, Boonstra T W and Breakspear M 2015 The heavy tail of the human brain *Curr. Opin. Neurobiol.* **31** 164–72

[3] Feliu E and Wiuf C 2012 Enzyme-sharing as a cause of multistationarity in signalling systems *J. R. Soc. Interface* **9** 1224–32

[4] Sabouri-Ghomi M, Ciliberto A, Kar S, Novak B and Tyson J J 2008 Antagonism and bistability in protein interaction networks *J. Theor. Biol.* **250** 209–18

[5] Straube R and Conradi C 2013 Reciprocal enzyme regulation as a source of bistability in covalent modification cycles *J. Theor. Biol.* **330** 56–74

[6] Ladewig J, Koch P and Brustle O 2013 Leveling waddington: the emergence of direct programming and the loss of cell fate hierarchies *Nat. Rev. Mol. Cell Biol.* **14** 225–36

[7] Elf J, Nilsson K, Tenson T and Ehrenberg M 2006 Bistable bacterial growth rate in response to antibiotics with low membrane permeability *Phys. Rev. Lett.* **97** 258104

[8] Meredith H R, Srimani J K, Lee A J, Lopatkin A J and You L 2015 Collective antibiotic tolerance: mechanisms, dynamics and intervention *Nat. Chem. Biol.* **11** 182–8

[9] Veening J W, Smits W K and Kuipers O P 2008 Bistability, epigenetics, and bet-hedging in bacteria *Annu. Rev. Microbiol.* **62** 193–210

[10] Guerrero P, Byrne H M, Maini P K and Alarcon T 2015 From invasion to latency: intracellular noise and cell motility as key controls of the competition between resource-limited cellular populations *J. Math. Biol.* 1–34

[11] Cinquin O and Demongeot J 2002 Positive and negative feedback: striking a balance between necessary antagonists *J. Theor. Biol.* **216** 229–41

[12] MacArthur B D *et al* 2012 Nanog-dependent feedback loops regulate murine embryonic stem cell heterogeneity *Nat. Cell Biol.* **14** 1139–47

[13] Housden B E and Perrimon N 2014 Spatial and temporal organization of signaling pathways *Trends Biochem. Sci.* **39** 457–64

[14] Cherry J L and Adler F R 2000 How to make a biological switch *J. Theor. Biol.* **203** 117–33

[15] Angeli D, Ferrell J E Jr and Sontag E D 2004 Detection of multistability, bifurcations, and hysteresis in a large class of biological positive-feedback systems *Proc. Natl Acad. Sci. USA* **101** 1822–7

[16] Gardner T S, Cantor C R and Collins J J 2000 Construction of a genetic toggle switch in *Escherichia coli Nature* **403** 339–42

[17] Hermsen R, Erickson D W and Hwa T 2011 Speed, sensitivity, and bistability in auto-activating signaling circuits *PLoS Comput. Biol.* **7** e1002265

[18] Diambra L, Senthivel V R, Menendez D B and Isalan M 2015 Cooperativity to increase turing pattern space for synthetic biology *ACS Synth. Biol.* **4** 177–86

[19] Buchler N E and Cross F R 2009 Protein sequestration generates a flexible ultrasensitive response in a genetic network *Mol. Syst. Biol.* **5** 272

[20] Buchler N E and Louis M 2008 Molecular titration and ultrasensitivity in regulatory networks *J. Mol. Biol.* **384** 1106–19

[21] Ferrell J E Jr and Ha S H 2014 Ultrasensitivity: III. Cascades, bistable switches, and oscillators *Trends Biochem. Sci.* **39** 612–8

[22] Kuznetsov Y A 1998 *Elements of Applied Bifurcation Theory* (New York: Springer)

[23] Buetti-Dinh A, Ungricht R, Kelemen J Z, Shetty C, Ratna P and Becskei A 2009 Control and signal processing by transcriptional interference *Mol. Syst. Biol.* **5** 300

[24] Carey L B, van Dijk D, Sloot P M, Kaandorp J A and Segal E 2013 Promoter sequence determines the relationship between expression level and noise *PloS Biol.* **11** e1001528

[25] Prabakaran S, Gunawardena J and Sontag E 2014 Paradoxical results in perturbation-based signaling network reconstruction *Biophys. J.* **106** 2720–8

[26] Hsu C, Scherrer S, Buetti-Dinh A, Ratna P, Pizzolato J, Jaquet V and Becskei A 2012 Stochastic signalling rewires the interaction map of a multiple feedback network during yeast evolution *Nat. Commun.* **3** 682

[27] Segel L A 1980 *Mathematical Models in Molecular and Cellular Biology* (Cambridge: Cambridge University Press)

[28] Tiwari A and Igoshin O A 2012 Coupling between feedback loops in autoregulatory networks affects bistability range, open-loop gain and switching times *Phys. Biol.* **9** 055003

[29] Siegal-Gaskins D, Mejia-Guerra M K, Smith G D and Grotewold E 2011 Emergence of switch-like behavior in a large family of simple biochemical networks *PLoS Comput. Biol.* **7** e1002039

[30] Chen D and Arkin A P 2012 Sequestration-based bistability enables tuning of the switching boundaries and design of a latch *Mol. Syst. Biol.* **8** 620

[31] Kelemen J Z, Ratna P, Scherrer S and Becskei A 2010 Spatial epigenetic control of mono- and bistable gene expression *PLoS Biol.* **8** e1000332

[32] Zerihun M B, Vaillant C and Jost D 2015 Effect of replication on epigenetic memory and consequences on gene transcription *Phys. Biol.* **12** 026007
[33] Taute K M, Gude S, Nghe P and Tans S J 2014 Evolutionary constraints in variable environments, from proteins to networks *Trends Genetics* **30** 192–8
[34] Meyer J R, Gudelj I and Beardmore R 2015 Biophysical mechanisms that maintain biodiversity through trade-offs *Nat. Commun.* **6** 6278
[35] de Visser J A G M and Krug J 2014 Empirical fitness landscapes and the predictability of evolution *Nat. Rev. Genetics* **15** 480–90
[36] Siuti P, Yazbek J and Lu T K 2014 Engineering genetic circuits that compute and remember *Nat. Protocols* **9** 1292–300
[37] Bonde M M, Voegeli S, Baudrimont A, Seraphin B and Becskei A 2014 Quantification of pre-mRNA escape rate and synergy in splicing *Nucleic Acids Res.* **42** 12847–60
[38] Martin-Perez M and Villen J 2015 Feasibility of protein turnover studies in prototroph *Saccharomyces cerevisiae* strains *Anal. Chem.* **87** 4008–14
[39] Tchourine K, Poultney C S, Wang L, Silva G M, Manohar S, Mueller C L, Bonneau R and Vogel C 2014 One third of dynamic protein expression profiles can be predicted by a simple rate equation *Mol. Biosyst.* **10** 2850–62
[40] Picotti P, Bodenmiller B, Mueller L N, Domon B and Aebersold R 2009 Full dynamic range proteome analysis of *S. cerevisiae* by targeted proteomics *Cell* **138** 795–806
[41] Koren R and Hammes G G 1976 A kinetic study of protein–protein interactions *Biochemistry* **15** 1165–71